



## Experimental study on thermal properties of foamed concrete with expanded perlite aggregate particle size and gradation

Yandong Liu<sup>a,b</sup>, Lingyonxg Ma<sup>a,b,\*\*</sup>, Wei Jiang<sup>b,c,\*</sup>, Qing Li<sup>a,b</sup>, Ming Qiao<sup>a,b</sup>, Shijie Fan<sup>a,b</sup>, Dong Li<sup>a,b</sup>

<sup>a</sup> School of Civil Engineering and Architecture, Northeast Petroleum University, Fazhan Lu Street, Daqing, 163318, China

<sup>b</sup> Heilongjiang Provincial Key Laboratory of Thermal Utilization and Disaster Reduction of New Energy in Cold Regions, Fazhan Lu Street, Daqing, 163318, China

<sup>c</sup> College of Civil Engineering and Water Conservancy, Heilongjiang Bayi Agricultural University, Xinfeng Lu Street, Daqing, 163319, China



### ARTICLE INFO

#### Keywords:

Expanded perlite foamed concrete  
Aggregate grading  
Compressive strength  
Thermal conductivity

### ABSTRACT

This study aimed to enhance the comprehensive properties of foamed concrete by using expanded perlite as the main aggregate. The study systematically examined the effects of water-cement ratio (0.6, 0.7, 0.8), single expanded perlite aggregate particle size (0.3–0.5 mm, 0.5–1 mm, 1–3 mm), and multi-particle size combinations (based on the Andreasen-Andersen equation, grading index q of 0.2, 0.3, 0.4). The effects of these factors on dry density, water absorption, compressive strength, thermal conductivity, and microstructure were evaluated against a conventional foamed concrete sample used as the control group. Experimental findings indicated that an elevated water-cement ratio notably decreased the dry density of the foamed concrete and increased water absorption, accompanied by a declining trend in compressive strength. Regarding mechanical strength, the 0.5–1 mm single expanded perlite aggregate achieved the highest compressive strength (9.12 MPa at w/c 0.6), while the 30:40:30 multi-particle size blend showed the second highest strength (8.06 MPa). For thermal performance, a low conductivity of 0.1194 W/(m·K) was obtained with a multi-particle size combination at a water-cement ratio of 0.8. This low conductivity was associated with a uniform vesicle distribution and dense pore structure. Incorporating expanded perlite aggregate significantly enhanced the dry density and compressive strength compared to control samples, while generally resulting in lower water absorption and higher thermal conductivity at the same water-cement ratio. Optimizing expanded perlite aggregate particle size and grading improves the mechanical strength of foamed concrete while maintaining its lightweight and thermal insulation properties.

### 1. Introduction

As human society advances, energy consumption has risen proportionally [1–3]. Persistent dependence on fossil fuels has intensified environmental challenges, attracting increasing attention from researchers and policymakers in recent years. The key to energy

\* Corresponding author. College of Civil Engineering and Water Conservancy, Heilongjiang Bayi Agricultural University, Xinfeng Lu Street, Daqing 163319, China.

\*\* Corresponding author. School of Civil Engineering and Architecture, Northeast Petroleum University, Fazhan Lu Street, Daqing, 163318, China.

E-mail addresses: [laomadaqing@qq.com](mailto:laomadaqing@qq.com) (L. Ma), [jiangwei429@126.com](mailto:jiangwei429@126.com) (W. Jiang).

saving and consumption reduction in the field of construction lies in scientifically and significantly reducing total building energy use. Building thermal insulation is a vital energy-saving method. It reduces the demand for heating and cooling by improving the thermal performance of structures. This enhances energy efficiency, lowers carbon emissions, and supports environmental protection and sustainable development [4–8].

Foamed concrete is a porous, lightweight cementitious material composed of cementitious materials, chemical admixtures, foam stabilizers, and foaming agents mixed in specific proportions [9]. It is characterized by low thermal conductivity, light weight, excellent seismic resistance, and superior fire performance, making it widely applicable in external wall insulation, cavity filling, shock-absorption barriers, and fire insulation systems [10,11]. To further enhance the mechanical properties and functionality of foamed concrete, the incorporation of various lightweight aggregates has become a major research focus. Among numerous lightweight aggregates, expanded perlite (EP) has garnered significant attention due to its unique comprehensive advantages. Expanded perlite is renowned not only for being lightweight, thermally insulating, environmentally friendly, and durable [12] but also for its considerable potential in improving the life-cycle energy efficiency of buildings. Compared to other lightweight aggregates (e.g., pumice, expanded clay), the closed-cell microstructure of EP often results in superior thermal insulation performance at comparable densities [13]. More importantly, its production typically entails lower embodied energy than sintered lightweight aggregates (e.g., expanded clay) [12], while the lightweighting effect it imparts can significantly reduce material consumption in foundational structures and transportation energy, achieving energy savings at the source. Therefore, incorporating expanded perlite into foamed concrete is not only an effective method to improve material properties but also a strategic choice aimed at enhancing the overall energy efficiency of buildings and reducing operational carbon emissions, holding significant importance for advancing green building practices. Recently, a series of studies concerning the application of expanded perlite in foamed concrete has been conducted by scholars, Demirboğa et al. [14], for example, studied the effect of mineral admixtures on the thermal and mechanical properties of expanded perlite aggregate concrete. The study's findings indicated that replacing Portland cement with mineral admixtures (e.g., silica fume and fly ash) led to a reduction in the thermal conductivity and density of concrete. The study by Sengul et al. [15] on lightweight concrete showed that increasing expanded perlite dosage resulted in a reduction in compressive strength and modulus of elasticity, alongside an increase in water absorption and permeability coefficient. Wang et al.'s study [16] demonstrated that a graded aggregate mix using 100 % of the new aggregate achieved an exceptionally low thermal conductivity of 0.098 W/(m•K) (with a compressive strength of 3.71 MPa), despite the new aggregate leading to reductions in overall concrete strength and thermal conductivity. Ibrahim et al. [17] established a process for preparing lightweight concrete (LWC) using expanded perlite aggregate and extensively evaluated its properties. The results showed that LWC significantly reduced weight by 20–30 % compared to normal concrete and its strength was satisfactory for structural applications. Grzeszczyk et al. [18] reported that incorporating 30 % expanded perlite into reactive powder concrete yielded a lightweight, high-strength concrete exhibiting a density of approximately 1900 kg/m<sup>3</sup>, a compressive strength exceeding 70 MPa, and minimal water absorption. In order to cost-effectively enhance the performance of cementitious materials, Jia et al. [19] study explored the application of aerogel/expanded perlite composites (AEP). It was confirmed that the negative effect of AEP on the workability of freshly mixed materials could be effectively overcome by optimizing the cementitious materials and modifying AEP, but the modification process would slowed down the hydration process. A study by Alexa-Stratulat et al. [20] evaluated the potential application of expanded perlite aggregate (EPA) in cement mortars, aiming to achieve a breakthrough in natural aggregate replacement. The mechanical properties of cement mortar incorporating varying dosages of EPA were investigated in this experimental study under both room and elevated temperatures. At room temperature, replacing natural sand with EPA led to decreased mortar strength, yet its effect on the modulus of elasticity was minimal for dosages up to 20 %.

Although existing studies have extensively explored the application of expanded perlite in various cementitious materials and its influence on their macroscopic properties, its specific use as an aggregate within the lightweight porous system of foamed concrete presents a knowledge gap. Specifically, the systematic modulation of the material's comprehensive performance by the aggregate's particle size and gradation (particularly concerning the synergistic mechanical strength and thermal performance), as well as the related microscopic mechanisms, remain insufficiently investigated when expanded perlite is used in this context.

Additionally, sustainability factors are increasingly important when evaluating building materials. Although expanded perlite originates from natural volcanic rock, its production requires high-temperature expansion processing, which consumes significant energy and may increase carbon emissions. However, its incorporation into foam concrete effectively reduces structural self-weight, decreases cement usage, and enhances thermal insulation properties, thereby achieving energy savings and emission reductions throughout the building's entire lifecycle. Therefore, when evaluating the suitability of this material, it is essential to balance the environmental costs incurred during the production phase against the sustainability benefits realized during its application phase.

Addressing this gap, this study employs expanded perlite, well recognized for its thermal insulation properties, as the aggregate in foamed concrete. We systematically examine the effects of single particle sizes and multi-particle size gradations on key properties—including dry density, water absorption, compressive strength, and thermal conductivity—under different water–cement ratios, and elucidate the underlying mechanisms through microstructural analysis. The findings establish quantitative relationships between mix parameters and material performance, providing a theoretical basis for understanding the role of perlite gradation in pore structure development. At the same time, they offer practical guidance for mixture design to balance strength and insulation requirements, while highlighting potential challenges in system integration and standardization. This study therefore contributes both to the scientific understanding of perlite-based foamed concrete and to its engineering application in lightweight, energy-efficient, and sustainable construction.

## 2. Methodology

### 2.1. Experimental materials and equipments

In this experiment, the non-demolition molding plate casting cement produced by China Daqing Biqi Li Technology Development Co. was used as the main material. The weight ratios of the cement foam are shown in [Table 1](#). Hydrogen peroxide with a concentration of 30 % produced by the same manufacturer was used as the foaming agent. The experiment utilized commercially available expanded perlite (Henan Yixiang New Materials Co., Ltd.) compliant with GB/T 10303-2015, with its primary chemical composition shown in [Table 2](#).

The instruments used for the experiment included a WAW-1000 electro-hydraulic servo testing machine, a JTRG-III thermal conductivity meter, and a Nikon D7000 camera for photographing the cut surface of the test block.

### 2.2. Mix proportion

To systematically examine the effects of aggregate gradation and particle size on the performance of expanded perlite foamed concrete, 18 sets of mixing ratios were developed for this experiment. The test parameters included: water-cement ratio (0.6–0.8), expanded perlite aggregate particle size (0.3–3 mm), and aggregate particle size type (single particle size/multi-particle size combination). In this experiment, multi-size aggregates underwent gradation optimization following the Andreasen-Andersen curve [[21](#)]. [Table 3](#) summarizes the composition of each mixture.

The study not only explored particle size and grading patterns but also examined the compatibility and synergistic effects between expanded perlite and foamed cement matrix to enhance the engineering applicability of the results. Both materials share characteristics of porosity, lightweight properties, and rapid hydration hardening. Their integration not only facilitates synchronized hydration processes, reduces internal stresses and cracking risks, but also optimizes thermal insulation performance through complementary pore structures. Accordingly, the experimental design has addressed critical compatibility issues such as the impact of high aggregate water absorption on workability and interfacial bonding properties. These aspects will be analyzed in the discussion using specific data, aiming to provide a more comprehensive basis for formulating high-performance lightweight insulation materials.

The Andreasen-Andersen curve is an important tool for aggregate grading optimization. The core idea is to significantly reduce the void ratio in concrete mixtures by rationally distributing aggregates with different particle sizes, specifically by utilizing fine particles to fill the interstitial spaces among coarser ones, aiming to achieve the maximum packing density of the aggregate system. Its mathematical expression is:

$$P(D) = \frac{D^q - D_{\min}^q}{D_{\max}^q - D_{\min}^q} \quad (1)$$

where  $P(D)$  is the volume fraction of particles of a given size,  $D_{\min}$  and  $D_{\max}$  are the minimum and maximum particle sizes (mm) of the particles in the mixture, respectively, and  $q$  is the gradation index, which controls the shape of the curve, reflecting the relative content of fine, medium and coarse aggregates.

### 2.3. Specimen preparation

The specimen preparation process is illustrated in [Fig. 1](#). The raw materials such as cement and expanded perlite were manually stirred in a dry container for 2 min, and then the premix and water were added into a cement paste mixer according to the preset water-cement ratio and stirred for 3 min to obtain the initial cement slurry. Subsequently, the foaming agent was added to the fresh slurry, and mixing proceeded for a duration of 2.5 min. Once mixing concluded, the fresh slurry was cast into 100 mm × 100 mm × 100 mm molds, with the specimens remaining in the molds for 24 h prior to demolding. All specimens were subjected to performance tests after curing for 28 d in a standard curing box at (20 ± 2) °C and 95 % relative humidity (as shown in [Fig. 2](#)).

### 2.4. Test methods

#### 2.4.1. Dry density and water absorption

The dry density and water absorption of expanded perlite foamed concrete specimens were measured by the weighing method in this study. Dry density was determined by drying specimens (cured to the specified age) in an oven until constant mass and then recording the dry mass. Following this, the volume of the specimen was determined by measuring its length, width, and height. The formula used for this calculation is provided below:

**Table 1**

Foamed cement specimen proportioning.

Ordinary silicate cement/%	Fast-hardening sulfoaluminate cement/%	Coal ash/%	Silica fume/%	Calcium stearate/%	Dispersed latex powder/%	Engineered fibers/%	Water reducing agent/%
66.5	6.5	20	5	1	0.2	0.5	0.3

**Table 2**

The main component of expanded perlite.

SiO <sub>2</sub>	Fe <sub>2</sub> O <sub>3</sub>	CaO	Al <sub>2</sub> O <sub>3</sub>	MgO	K <sub>2</sub> O	Na <sub>2</sub> O
73.41	1.01	1.63	14.26	0.35	3.98	5.36

**Table 3**

Experimental group.

Experimental group	Water-cement ratio	Particle size type	Particle size (mm)	Proportion (%)	Gradation index
C <sub>0.6-S-0.3</sub>	0.6	Single size	0.3–0.5	100	—
C <sub>0.6-S-0.5</sub>	0.6	Single size	0.5–1	100	—
C <sub>0.6-S-1</sub>	0.6	Single size	1–3	100	—
C <sub>0.6-M-0.2</sub>	0.6	Multi-size	0.3–0.5, 0.5–1, 1–3	30, 40, 30	0.2
C <sub>0.6-M-0.3</sub>	0.6	Multi-size	0.3–0.5, 0.5–1, 1–3	30, 30, 40	0.3
C <sub>0.6-M-0.4</sub>	0.6	Multi-size	0.3–0.5, 0.5–1, 1–3	20, 30, 50	0.4
C <sub>0.7-S-0.3</sub>	0.7	Single size	0.3–0.5	100	—
C <sub>0.7-S-0.5</sub>	0.7	Single size	0.5–1	100	—
C <sub>0.7-S-1</sub>	0.7	Single size	1–3	100	—
C <sub>0.7-M-0.2</sub>	0.7	Multi-size	0.3–0.5, 0.5–1, 1–3	30, 40, 30	0.2
C <sub>0.7-M-0.3</sub>	0.7	Multi-size	0.3–0.5, 0.5–1, 1–3	30, 30, 40	0.3
C <sub>0.7-M-0.4</sub>	0.7	Multi-size	0.3–0.5, 0.5–1, 1–3	20, 30, 50	0.4
C <sub>0.8-S-0.3</sub>	0.8	Single size	0.3–0.5	100	—
C <sub>0.8-S-0.5</sub>	0.8	Single size	0.5–1	100	—
C <sub>0.8-S-1</sub>	0.8	Single size	1–3	100	—
C <sub>0.8-M-0.2</sub>	0.8	Multi-size	0.3–0.5, 0.5–1, 1–3	30, 40, 30	0.2
C <sub>0.8-M-0.3</sub>	0.8	Multi-size	0.3–0.5, 0.5–1, 1–3	30, 30, 40	0.3
C <sub>0.8-M-0.4</sub>	0.8	Multi-size	0.3–0.5, 0.5–1, 1–3	20, 30, 50	0.4

Note: The label consists of the material type (C-foamed concrete), water-cement ratio (e.g., 0.6), particle size type (S-single particle size, M-multiple particle size combination), minimum particle size (0.3), and grading index q-value (e.g., 0.2).

$$\rho = \frac{m}{V} \quad (2)$$

where  $\rho$  is the dry density,  $m$  is the dry weight, and  $V$  is the volume of the specimen.

Following the dry density measurement, water absorption was determined. Dried specimens were submerged in water until constant mass was achieved (saturation). The saturated mass was recorded immediately after removing surface water with a damp cloth. The calculation utilized the formula below:

$$W = \frac{m_1 - m_0}{m_0} \times 100 \quad (3)$$

where  $W$  is the water absorption rate,  $m_0$  is the mass of the specimen before immersion,  $m_1$  is the mass of the specimen after saturation.

#### 2.4.2. Compressive strength

Compressive strength was tested following the procedure outlined in the ASTM C 495 standard [22]. Fig. 3 shows the device used for determining the compressive strength of the specimens.

#### 2.4.3. Thermal conductivity

The ASTM C 518 standard [23] was followed to determine the thermal conductivity of the foamed concrete. Foam concrete panels with dimensions of 300 mm × 300 mm × 30 mm were used for the thermal conductivity test. After the cured specimens were oven-dried to constant mass, thermal conductivity was measured. The value presented represents the average of three specimens and has a reported accuracy of 0.001 W/(m·K).

#### 2.4.4. Microstructure analysis

For microstructural analysis, the specimens were sectioned along the cross-section and the sections were ground and polished using sandpaper to obtain a flat viewing surface. Subsequently, a camera was used to obtain cross-sectional images of the specimens and they were binarized in black and white using image processing software (Photoshop).

#### 2.5. Limitations and challenges of experimental methods and the influence of external factors

Although the experimental methods employed in this study were meticulously designed to evaluate the impact of expanded perlite on the properties of foam concrete, certain limitations exist, and external factors may influence the experimental results.

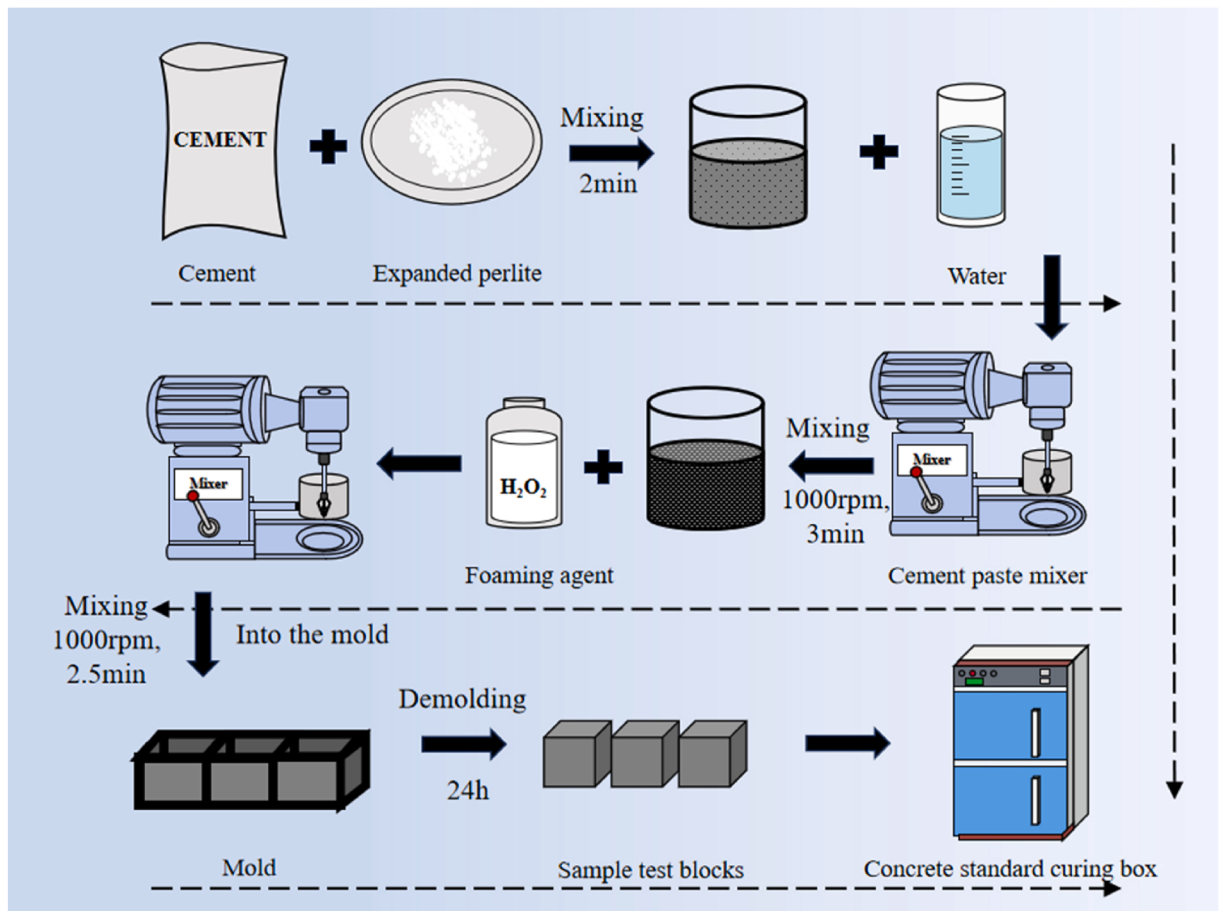


Fig. 1. Test block preparation procedure.



Fig. 2. Specimen samples.



**Fig. 3.** WAW-1000 electro-hydraulic servo testing machine.

- (1) Sample Size and Representativeness: The 18 experimental samples used in this study may not fully represent all concrete mix designs. Future research will increase the sample size and expand the range of mix designs.
- (2) Environmental Conditions: Temperature and humidity may affect concrete hardening processes. Although experiments were conducted under standard conditions, minor environmental fluctuations could still influence results. Future studies will therefore implement stricter environmental control.
- (3) Material Variability: Batch differences in expanded perlite and other materials may impact experimental outcomes. Despite controlling material usage, batch variations remain a significant factor.
- (4) Particle Size Distribution: The distribution of multiple particle size combinations may be uneven, affecting concrete performance. Future research will enhance result accuracy by optimizing particle distribution.
- (5) Testing Precision: Instrumental precision may introduce errors, particularly in thermal conductivity testing where temperature gradients and sample size variations can impact results. Future studies will reduce errors through multiple tests or higher-precision instruments.
- (6) Moisture Content and Thermal Conductivity: Thermal conductivity was measured in a dried state to minimize uncertainties caused by moisture fluctuations and ensure comparability between formulations. It should be noted, however, that the thermal conductivity of dried specimens typically represents the lowest value, whereas materials in actual engineering applications, subjected to ambient humidity conditions, often exhibit higher thermal conductivity. Previous studies indicate that thermal conductivity increases significantly with rising moisture content. This occurs because water's thermal conductivity (approximately 0.6 W/m·K) is substantially higher than that of air (approximately 0.025 W/m·K), and moisture filling pores weakens thermal insulation performance (Nguyen et al., 2017; Mydin et al., 2023 [24,25]). Therefore, the results presented herein should be regarded as baseline values for materials under optimal thermal insulation conditions. Future studies will consider testing under equilibrium moisture conditions to better reflect practical applications.

In summary, despite our best efforts to control various factors in the experiment, external elements such as environmental conditions, variations in material properties, and experimental procedures may still exert potential influences on the results. Therefore, future research should meticulously account for these external factors and further enhance the robustness and reliability of experimental outcomes by optimizing experimental design and operational protocols.

**Table 4**

Test group without added expanded perlite.

Specimen	Water-cement ratio	Dry density/(kg·m <sup>-3</sup> )	Water Absorption(%)	Compressive strength (MPa)	Thermal conductivity (W/(m·K))
C <sub>0.6-Origin</sub>	0.6	832.7	23	2.89	0.1401
C <sub>0.7-Origin</sub>	0.7	744.6	28	1.93	0.0829
C <sub>0.8-Origin</sub>	0.8	658.0	32	1.33	0.0931

Note: The benchmark samples are labeled by material type (C-foamed concrete), water-cement ratio (e.g., 0.6), and a suffix (-Origin) indicating the absence of expanded perlite aggregate.

### 3. Results and discussion

#### 3.1. Benchmark performance of conventional foamed concrete

To assess the specific effect of expanded perlite aggregate on the performance of foamed concrete and highlight the innovative nature of this study, this section initially presents performance data for conventional chemically foamed concrete without expanded perlite. These data serve as a benchmark for comparison and were obtained from experimental results where the water/cement ratio (W/C) was varied using the same type of base cementitious material system lacking expanded perlite aggregate, as detailed in [Table 4](#).

As evident from [Table 4](#) the water-cement ratio significantly impacts the characteristics of conventional foamed concrete. Increasing the water-cement ratio from 0.6 to 0.8 causes a substantial decrease in the material's dry density, from 832.7 kg/m<sup>3</sup> to 658.0 kg/m<sup>3</sup>, thereby increasing its lightness. However, this reduction in density is associated with performance compromises: water absorption rises sharply from 23 % to 32 %, demonstrating how increased porosity leads to higher water uptake capacity; simultaneously, compressive strength drops rapidly from 2.89 MPa to 1.33 MPa, illustrating the adverse effect of an elevated water-cement ratio on mechanical performance. Concerning thermal properties, thermal conductivity shows an initial decrease followed by a slight increase with rising water-cement ratio. The lowest value, 0.0829 W/(m-K), is recorded at a water-cement ratio of 0.7, corresponding to a dry density of 744.6 kg/m<sup>3</sup> and a compressive strength of 1.93 MPa. This indicates that significant intrinsic trade-offs exist when optimizing the performance of pure cement-based chemical foams without solid aggregates. While a balance between lightness, thermal insulation, and mechanical strength can be achieved within a certain range by adjusting foaming parameters such as the water-cement ratio, pursuing excessively low densities often weakens the material's structural integrity, resulting in a significant reduction in compressive strength.

Drawing from the data presented in [Table 4](#), and with particular consideration for the basic strength requirements in certain foamed concrete applications, the set of properties achieved at a water-cement ratio of 0.7 (dry density: 744.6 kg/m<sup>3</sup>, compressive strength: 1.93 MPa, thermal conductivity: 0.0829 W/(m-K)) serves as a crucial reference benchmark for evaluating the impact of incorporating expanded perlite aggregates in this study. The influence of varying expanded perlite aggregate particle sizes, gradations, and water-cement ratios on foamed concrete performance will be discussed in detail in the subsequent sections. Comparative analyses will be conducted against these benchmark values to reveal the specific effects and potential for performance optimization stemming from the incorporation of expanded perlite aggregate.

#### 3.2. Dry density and water absorption

This study investigated the water absorption characteristics of expanded perlite foamed concrete across varying dry densities, achieved by manipulating the water-cement ratios (0.6, 0.7, and 0.8). Analysis of the experimental data ([Table 5](#) and [Fig. 4](#)) revealed a significant decrease in dry density and a notable increase in water absorption with increasing water-cement ratio.

[Table 5](#) demonstrates that the dry density of foamed concrete decreases significantly as the water-cement ratio increases. At a water-cement ratio of 0.6, the average dry density was 1130.6 kg/m<sup>3</sup>. With further increases in the water-cement ratio to 0.7 and 0.8, the dry density reduced to 1074.5 kg/m<sup>3</sup> and 972.5 kg/m<sup>3</sup>, respectively. Relative to the plain foamed concrete benchmark ([Table 4](#)), the inclusion of expanded perlite aggregate significantly increased the dry density of the foamed concrete at equivalent water-cement ratios. For instance, at a water-cement ratio of 0.6, the benchmark group exhibited a dry density of 832.7 kg/m<sup>3</sup> (C<sub>0.6-Origin</sub>), whereas the average dry density rose to 1130.6 kg/m<sup>3</sup> with expanded perlite incorporation. Similarly, at a water-cement ratio of 0.7, the baseline dry density was 744.6 kg/m<sup>3</sup> (C<sub>0.7-Origin</sub>), while the average dry density reached approximately 1074.5 kg/m<sup>3</sup> after expanded perlite addition. Likewise, at a water-cement ratio of 0.8, the baseline density was 658.0 kg/m<sup>3</sup> (C<sub>0.8-Origin</sub>), compared to approximately 972.5 kg/m<sup>3</sup> for the expanded perlite foamed concrete. This indicates that expanded perlite aggregate is intrinsically denser than the pure foam pores, and its incorporation elevates the solid mass per unit volume of the material. Notably, at a given water-cement ratio, variations in expanded perlite aggregate particle size and gradation also influence the material's final dry density ([Table 5](#)), which is attributed to the varying stacking characteristics of the aggregates and their corresponding cement paste demand for encapsulation.

[Fig. 4](#) illustrates the variation in water absorption for expanded perlite foamed concrete across different water-cement ratios. The results indicate that water absorption increases significantly as the water-cement ratio rises. In comparison with the baseline data ([Table 4](#)), the foamed concrete incorporating expanded perlite aggregate generally exhibited lower water absorption at equivalent water-cement ratios. Specifically, at a water-cement ratio of 0.8, the benchmark group (C<sub>0.8-Origin</sub>) showed a water absorption of 32 %,

**Table 5**

Foamed concrete dry density.

Specimen	Dry density/(kg/m <sup>3</sup> )	Specimen	Dry density/(kg/m <sup>3</sup> )	Specimen	Dry density/(kg/m <sup>3</sup> )
C <sub>0.6-S-0.3</sub>	916.4	C <sub>0.7-S-0.3</sub>	949.6	C <sub>0.8-S-0.3</sub>	815.3
C <sub>0.6-S-0.5</sub>	1274.0	C <sub>0.7-S-0.5</sub>	1154.4	C <sub>0.8-S-0.5</sub>	1096.7
C <sub>0.6-S-1</sub>	1171.7	C <sub>0.7-S-1</sub>	1050.5	C <sub>0.8-S-1</sub>	900.6
C <sub>0.6-M-0.2</sub>	1209.1	C <sub>0.7-M-0.2</sub>	1110.9	C <sub>0.8-M-0.2</sub>	1054.4
C <sub>0.6-M-0.3</sub>	1096.3	C <sub>0.7-M-0.3</sub>	1064.1	C <sub>0.8-M-0.3</sub>	916.4
C <sub>0.6-M-0.4</sub>	1116.5	C <sub>0.7-M-0.4</sub>	1117.6	C <sub>0.8-M-0.4</sub>	1051.7

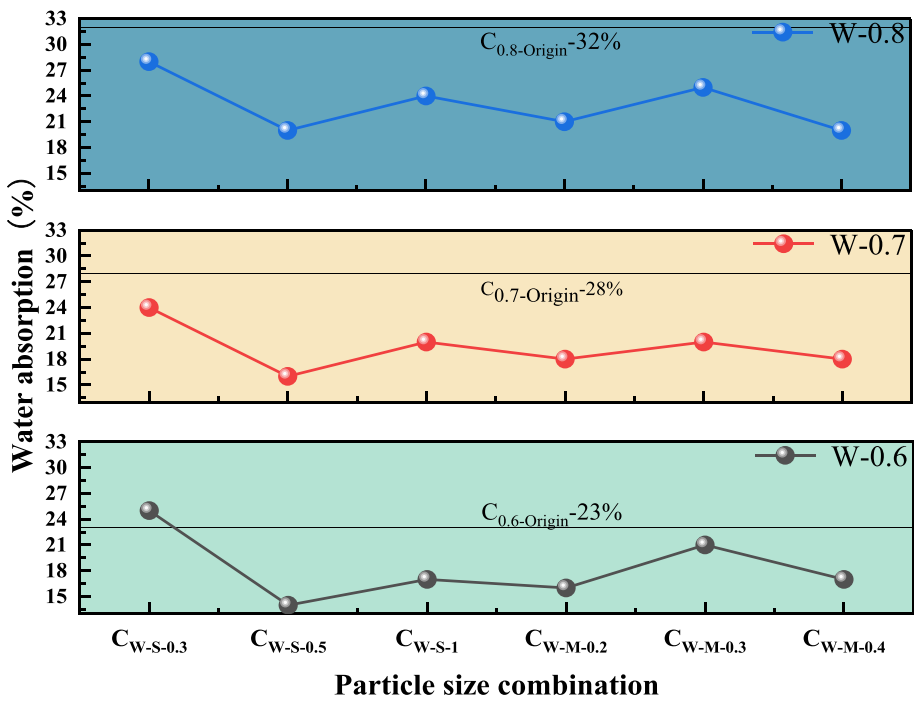


Fig. 4. Foamed concrete water absorption.

whereas the range for the expanded perlite foamed concrete test groups was approximately 21 %–25 % (see C<sub>0.8</sub> series in Fig. 4), a value significantly lower than that of the benchmark. This is attributed to a reduction in the number of connecting pores and the connectivity of the pore network, resulting in relatively lower water absorption, even with the material's increased overall density.

Experimental findings indicate that the water-cement ratio critically influences the dry density and water absorption of expanded perlite foamed concrete. An elevated water-cement ratio primarily reduces dry density owing to the dilution of the cementitious paste

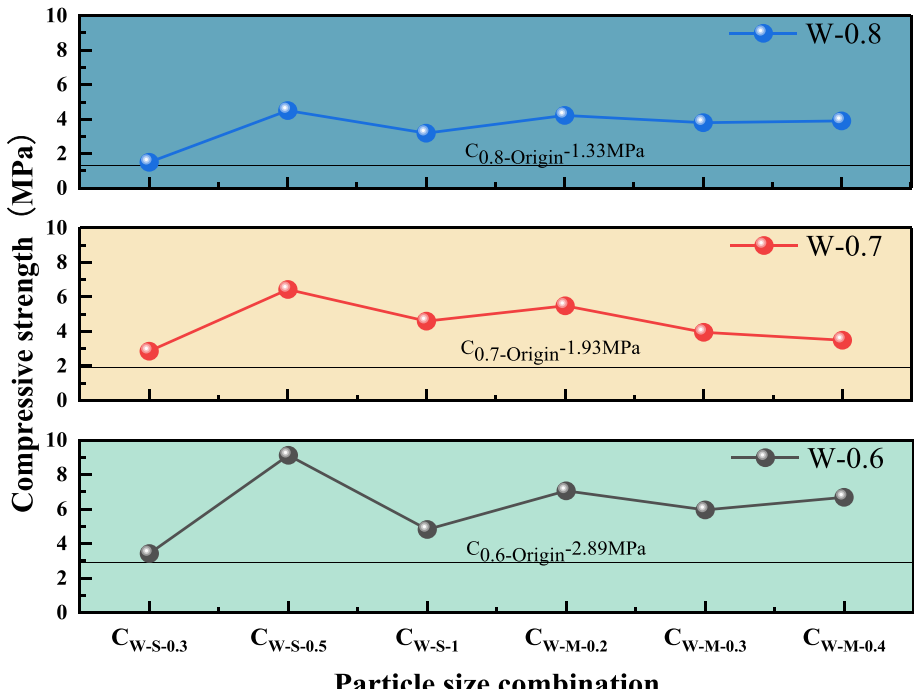


Fig. 5. Foamed concrete compressive strength.

and reduced solid phase volume [26,27]. Simultaneously, elevated water-cement ratios also increase the internal porosity of the foamed concrete, which can include localized voids resulting from uneven aggregate dispersion, ultimately leading to increased water absorption.

### 3.3. Compressive strength

**Fig. 5** presents the compressive strength of expanded perlite foamed concrete across different water-cement ratios (0.6, 0.7, and 0.8), examining the influence of single particle sizes (0.3–0.5 mm, 0.5–1 mm, and 1–3 mm) and multi-particle size combinations (30:40:30, 30:30:40, and 20:30:50). Results indicated that at a water-cement ratio of 0.6, the highest compressive strength of 9.12 MPa was achieved with the 0.5–1 mm particle size aggregate, followed by the 30:40:30 multi-particle size combination at 8.06 MPa (**Fig. 5**). These strength values significantly exceeded those of the benchmark test group without expanded perlite addition ( $C_{0.6\text{-Origin}}$ , 2.89 MPa) at the same water-cement ratio.

As illustrated in **Fig. 5**, a significant decay trend in compressive strength is observed as the water-cement ratio increases from 0.6 to 0.8. This phenomenon aligns with the fundamental principles of cementitious materials, where an increased water-cement ratio reduces the effective solid phase content of the cement matrix, consequently reducing the material's structural strength. Conversely, compared to the pure foamed concrete benchmark (**Table 4**), expanded perlite foamed concrete exhibited significantly higher compressive strength compared to plain foamed concrete (without aggregate addition) at all tested water-cement ratios. At a w/c ratio of 0.7, for example, expanded perlite foamed concrete achieved strengths ranging from 4.69 to 7.67 MPa, significantly exceeding the benchmark strength of 1.93 MPa. Findings suggest that expanded perlite aggregate markedly enhances the compressive strength of foamed concrete by building a stronger skeleton structure and providing improved load-bearing capacity.

Among the single expanded perlite aggregate sizes, the 0.5–1 mm fraction exhibited the best compressive performance consistently across all tested water-cement ratios. This suggests that within this size range, EP particles more effectively foster the formation of an optimal skeleton structure and significantly enhance the aggregate-cementitious matrix interfacial bond, thereby considerably enhancing the composite's load-bearing capacity [28–30]. Conversely, the 0.3–0.5 mm single aggregate exhibited the lowest compressive strength across all water-cement ratios. This is likely due to its high specific surface area, which promotes agglomeration and leads to poor dispersion within the cement paste.

Among the tested multi-particle size combinations, the 30:40:30 blend exhibited notable compressive strength. This is primarily attributed to its optimized particle size distribution, facilitating an effective synergy between strength and compactness. Within this multi-size aggregate blend, variously sized expanded perlite particles packed effectively, leading to a significant reduction in internal porosity. This enhanced the overall compactness of the foamed concrete and consequently boosted its compressive strength.

To validate the reliability of these observations, we conducted further statistical analysis. Results from one-way analysis of variance (ANOVA) indicated that under the same water-cement ratio, compressive strength differences among various particle size combinations were statistically significant ( $p < 0.05$ ). Two-way ANOVA further revealed that both the water-cement ratio and particle size

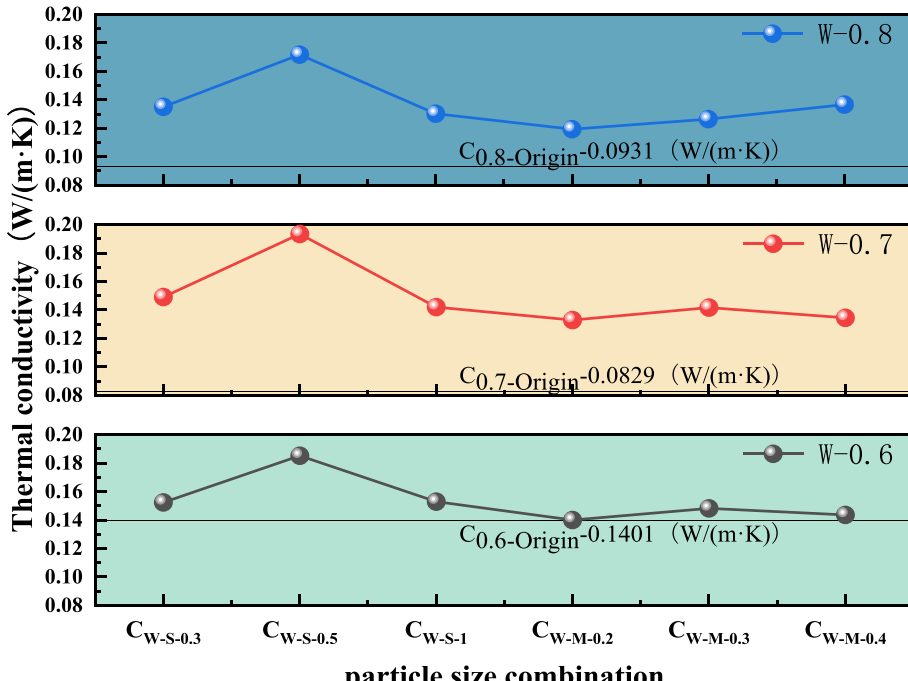


**Fig. 6.** Foamed concrete thermal conductivity.

distribution exerted significant main effects on compressive strength, with a significant interaction between the two factors ( $p < 0.05$ ). Post-hoc Tukey multiple comparison tests revealed that the 0.5–1 mm single-size group and the 30:40:30 multi-size combination exhibited significantly higher compressive strength than other groups. These results provide robust statistical evidence supporting the conclusions of this study, indicating that the observed differences were not random but resulted from the systematic effects of the mixed design parameters.

### 3.4. Thermal conductivity

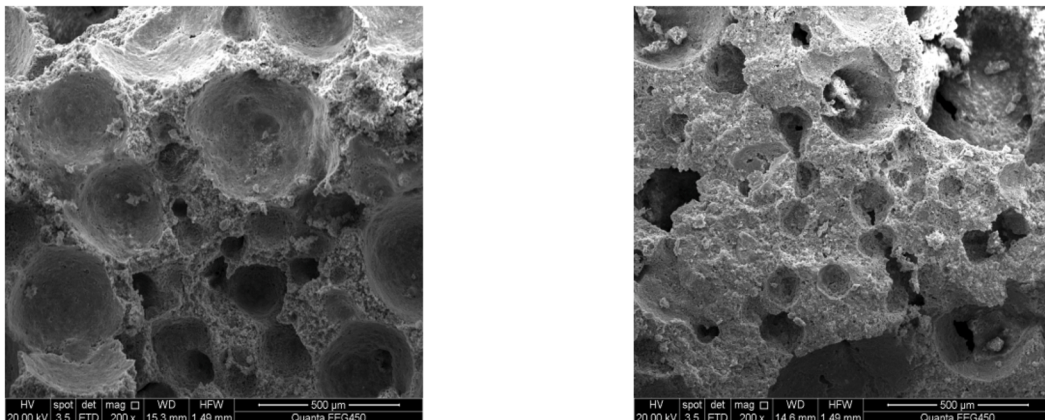
As displayed in Fig. 6, the thermal conductivity of expanded perlite foamed concrete decreases overall with increasing water-cement ratio (0.6–0.8). This trend indicates that lower water-cement ratios are less effective in reducing thermal conductivity, resulting in less favorable thermal insulation properties [31].

In comparison with the control group lacking expanded perlite (Table 4), the thermal conductivity of expanded perlite foamed concrete was generally higher. Specifically, the benchmark group achieved a value as low as 0.0829 W/(m·K) at a water-cement ratio of 0.7, compared to the thermal conductivity of expanded perlite foamed concrete, which was generally above 0.12 W/(m·K) (Fig. 6). This indicates that despite expanded perlite being a lightweight aggregate, its presence still increases the solid heat transfer paths, consequently diminishing the material's thermal insulation relative to a pure foam structure.

Experimental results reveal that expanded perlite particle size significantly affects the thermal conductivity of foamed concrete. The highest thermal conductivity (0.1934 W/(m·K)) occurs at the 0.5–1 mm particle size, whereas the lowest (0.1303 W/(m·K)) is observed for the 1–3 mm particle size. This is attributed to the fact that larger particle sizes create more air-containing pores within the foamed concrete, which effectively impede heat transfer, reflecting that expanded perlite particle size directly influences the pore structure and thus thermal conductivity [32].

Multi-particle size combinations of expanded perlite significantly lowered the thermal conductivity of foamed concrete, with experiments indicating that the thermal conductivity was typically below values obtained with single particle sizes. Notably, the 30:30:40 combination yielded the optimal thermal performance at a water-cement ratio of 0.7, achieving a thermal conductivity value of 0.1194 W/(m·K). This is likely due to the optimization of the pore structure resulting from the multi-particle size combination, with improved pore compactness achieved by the filling action of varying particle sizes and effectively reducing heat transfer paths, consequently improving the material's thermal insulation performance. It should be noted, however, that the minimum thermal conductivity obtained with expanded perlite foamed concrete (0.1194 W/(m·K)) remained higher than that of the benchmark test group (0.0829 W/(m·K)). This observation supports the conclusion that the inclusion of expanded perlite aggregate leads to a significant improvement in mechanical properties (Section 3.2), but with a trade-off in thermal insulation. Despite this, expanded perlite foamed concrete is still an excellent thermal insulation material while maintaining a certain level of strength compared to ordinary concrete or lightweight aggregate concrete of the same strength class.

Statistical analysis further validated the reliability of the aforementioned results. One-way analysis of variance (ANOVA) indicated statistically significant differences in thermal conductivity among the different particle size groups ( $p < 0.05$ ). Specifically, the lowest thermal conductivity of the 1–3 mm particle size group and the highest thermal conductivity of the 0.5–1 mm particle size group both exhibited significant differences compared to the other groups. Furthermore, the thermal conductivity of multi-particle-size combinations was significantly lower than that of single-particle-size groups ( $p < 0.05$ ). These findings provide robust statistical evidence supporting the conclusion that multi-gradation systematically optimizes pore structure and enhances thermal conductivity, indicating



(a)Foamed concrete without expanded perlite

(b)Microstructure of expanded perlite foamed concrete (Mix C<sub>0.7</sub>-M-0.2)

Fig. 7. Microstructure of foamed concrete.

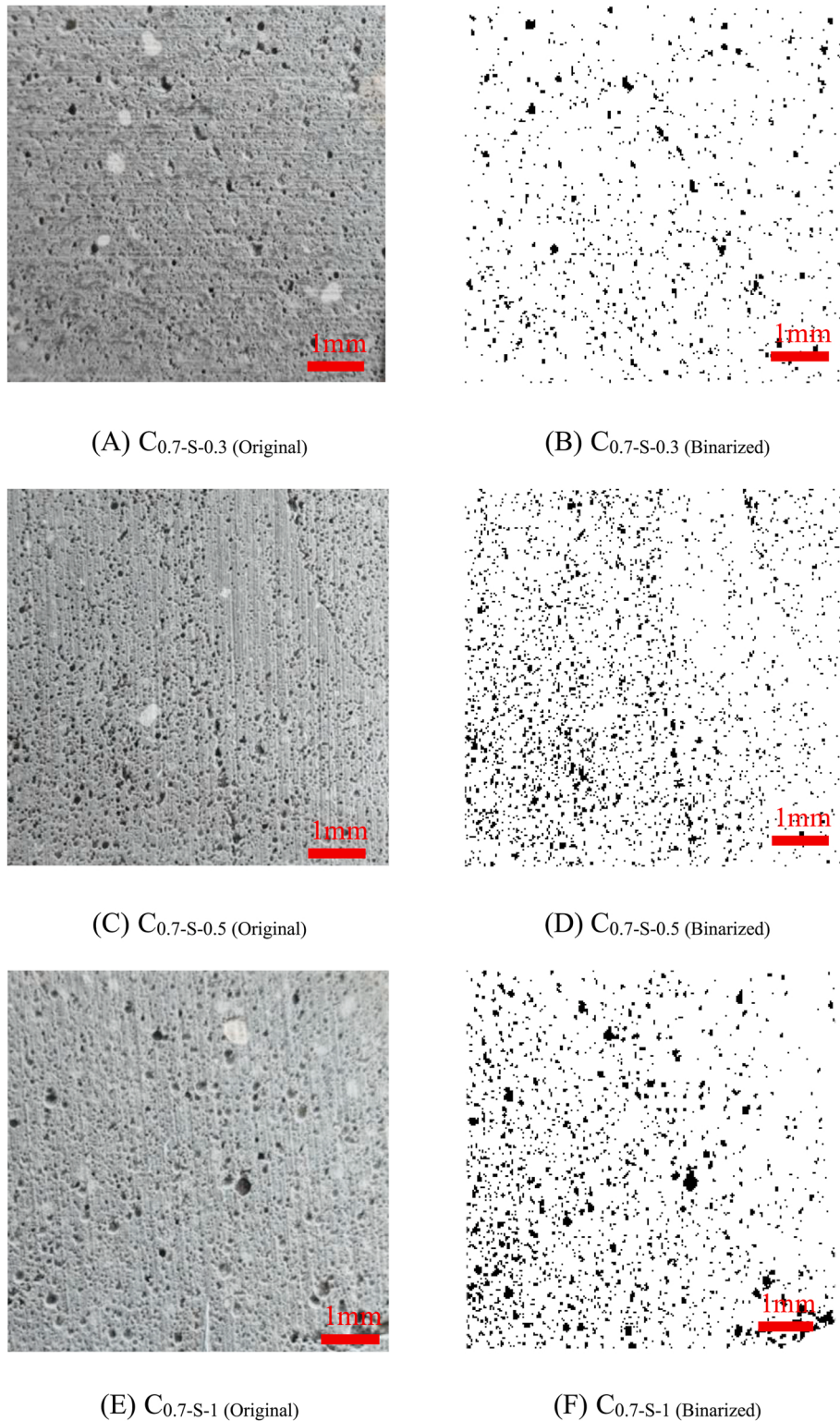


**Fig. 8.** The typical cross-sectional picture and its binary form.

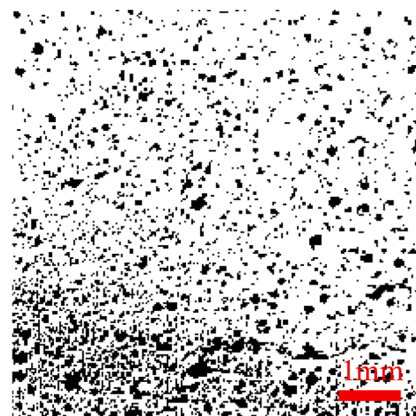
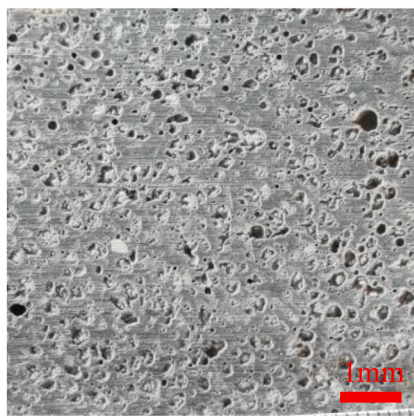
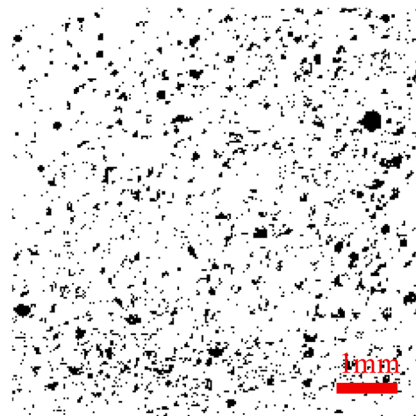
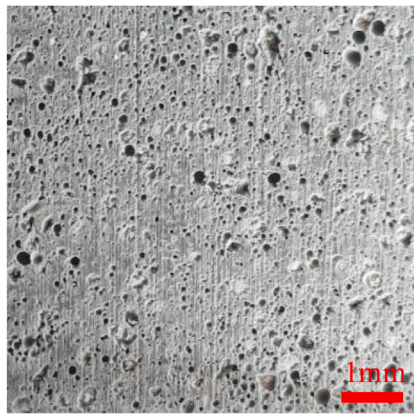
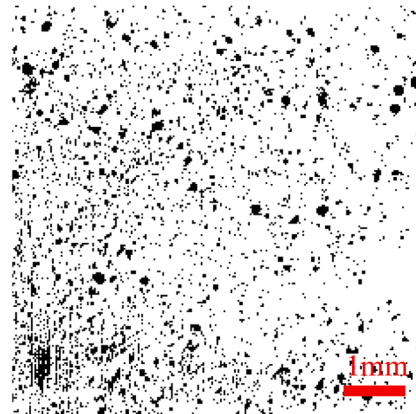
(G) C<sub>0.7</sub>-M-0.2 (Original)(H) C<sub>0.7</sub>-M-0.2 (Binarized)(I) C<sub>0.7</sub>-M-0.3 (Original)(J) C<sub>0.7</sub>-M-0.3 (Binarized)(K) C<sub>0.7</sub>-M-0.4 (Original)(L) C<sub>0.7</sub>-M-0.4 (Binarized)

Fig. 8. (continued).

that this effect is not attributable to random fluctuations.

### 3.5. Microstructure analysis

The microstructure plays a pivotal role in determining the macroscopic properties of foamed concrete. This study employed scanning electron microscopy (SEM) to comparatively analyze the microstructures of conventional foamed concrete (lacking expanded perlite) and expanded perlite foamed concrete, aiming to clarify the fundamental impact of expanded perlite incorporation on the material's structural morphology. As illustrated in Fig. 7(a) traditional foamed concrete displays a comparatively homogeneous skeletal pore structure, primarily composed of a continuous hardened cement matrix and uniformly dispersed, relatively regular macro-bubbles (foamed pores). Conversely, Fig. 7(b) clearly illustrates the complex composite microstructure of the material after expanded perlite aggregate is introduced, with irregularly shaped, porous expanded perlite particles effectively embedded within the foamed concrete matrix as discrete aggregate phases. Expanded perlite aggregates themselves have an inherent microporous structure, and an interfacial transition zone (ITZ) develops between the aggregate particles and the cement matrix, with the stacking of aggregate particles also contributing to the macroscopic pore network. Consequently, incorporating expanded perlite fundamentally changed the initial pore composition and distribution, limited to matrix and foamed pores, constructing a multi-level, multi-modal pore network that includes foamed pores, internal expanded perlite micropores, and aggregate gaps. Such a transformation at the microstructural level directly influences the material's bulk density, its heat conduction mechanisms, and mechanical load transfer paths, and thereby governs the differences and improvements observed in the macroscopic performance of expanded perlite foamed concrete compared to traditional foamed concrete.

Following the previous analysis, we further investigated the fine regulation of expanded perlite foamed concrete microstructure by the aggregate's own properties (particle size and gradation), with a representative sample at a water-cement ratio of 0.7 shown in Fig. 8. Microstructural analysis demonstrates that the particle size of expanded perlite plays a crucial role in regulating the pore structure [33]. The impact of single-size aggregates on pore structure varies with their dimension: smaller aggregates (e.g., 0.3–0.5 mm, Fig. 8(a)) promote the formation of fine and dense pores in the matrix, while larger aggregates (e.g., 1–3 mm, Fig. 8(E)) are associated with the formation of relatively large inter- or peri-aggregate pores. Nevertheless, single particle size aggregates make pore distribution optimization difficult because of their low stacking efficiency, potentially resulting in uneven pore size distribution or insufficiently dense aggregate packing (see C<sub>0.7-S</sub> series images in Fig. 8).

By contrast, a significant improvement in the pore structure of expanded perlite foamed concrete can be achieved by utilizing a multi-particle size combination strategy (see comparison of C<sub>0.7-S</sub> and C<sub>0.7-M</sub> series images in Fig. 8). The effective filling action of varying expanded perlite particle sizes promotes a more uniform dispersion of aggregates in the matrix and tighter aggregate stacking, resulting in a decreased macroscopic void ratio and a denser overall structure. Through optimization of the aggregate grading index (e.g., using Andreasen-Andersen curves), precise regulation of pore size and distribution becomes possible, leading to a more favorable microstructure. Fig. 8(H), for instance, shows that the 30:40:30 mix (C<sub>0.7-M-0.2</sub>), with a gradation index near 0.2, exhibits a more uniform and fine pore distribution and denser aggregate buildup compared to C<sub>0.7-M-0.3</sub> and C<sub>0.7-M-0.4</sub>. This is consistent with its superior mechanical and thermal properties at the corresponding water-cement ratio. This finding strongly supports the key role of expanded perlite aggregate grading optimization in governing the microstructure of foamed concrete and its macroscopic properties.

### 3.6. Economic performance and engineering application prospects

The results of this study demonstrate that the optimized expanded perlite foamed concrete (EP-FRC) exhibits not only excellent performance but also significant economic advantages and broad engineering application prospects. Its value can be quantitatively assessed through direct material costs and long-term energy-saving benefits.

#### 3.6.1. Direct material cost analysis

The economic advantage of EP-FRC stems from partially replacing the higher-cost foamed concrete base material with low-cost expanded perlite (approximately 40 CNY/m<sup>3</sup>). The substantial increase in strength (e.g., from 2.89 MPa in the benchmark group to 9.12 MPa, with a strength ratio  $n = 9.12/2.89 \approx 3.16$ ) is key. According to the principles of material mechanics, under bending loads, the relationship between load-bearing capacity and material strength can be simplified as:

$$M \propto f b h^2 \quad (4)$$

where  $M$  is the bending moment,  $f$  is the compressive strength, and  $bh^2$  is the thickness. To achieve the same load-bearing capacity (constant  $M$ ), when the strength increases by a factor of  $n$ , the theoretically required thickness  $h_{new}$  can be reduced to  $1/\sqrt{n}$  times the original thickness  $h_{orig}$ , i.e.:

$$h_{new} = \frac{h_{orig}}{\sqrt{n}} \quad (5)$$

With  $n = 3.16$ ,  $h_{new} \approx 0.56 h_{orig}$ . This implies that the material usage can be reduced by approximately 44 %. Although the unit volume cost of EP-FRC may increase slightly due to the addition of aggregate (e.g., assumed increase from 450 CNY/m<sup>3</sup> to 500 CNY/m<sup>3</sup>), the calculated unit area material cost  $C_{area}$  is:

$$C_{\text{area,EPC}} = 500 \text{CNY/m}^3 \times 0.56 h_{\text{orig}} = 280 h_{\text{orig}} \quad (6)$$

$$C_{\text{area,Orig}} = 450 \text{CNY/m}^3 \times h_{\text{orig}} = 450 h_{\text{orig}} \quad (7)$$

The comparison shows that the unit area material cost of EPC can be reduced by approximately 38 % compared to the benchmark sample, demonstrating direct economic benefits.

### 3.6.2. Long-term energy-saving benefit analysis

The thermal insulation performance of EP-FRC can be translated into significant operational energy savings. Its thermal conductivity is as low as, superior to ordinary concrete (0.1194 W/(m·K)). According to the steady-state heat transfer formula, the heat flux per unit area  $q$  is:

$$q = \frac{\lambda}{d} \Delta T \quad (8)$$

Where  $d$  is the thickness and  $\Delta T$  is the temperature difference between indoors and outdoors. Assuming application in an exterior wall with thickness  $d = 0.1$  m, a winter temperature difference, and a heating season of 120 days, the daily heat loss per unit area  $Q_{\text{daily}}$  for the EP-FRC wall is:

$$Q_{\text{daily,EPC}} = \frac{0.1194}{0.1} \times 20 \times 24 \times 3600 / 10^6 \approx 2.07 \text{kWh/m}^2 \quad (9)$$

Under the same conditions, the heat loss of an ordinary concrete wall ( $\lambda_c = 1.7$ ,  $d = 0.2$  m) would be approximately 14.7 kWh/m<sup>2</sup>. If the electricity price is 0.6 CNY/kWh, the energy-saving benefit per square meter of exterior wall during one heating season  $S_{\text{energy}}$  is:

$$S_{\text{energy}} = (14.7 - 2.07) \times 120 \times 0.6 \approx 908 \text{CNY/m}^2 \quad (10)$$

This highlights its substantial long-term economic value.

### 3.6.3. Engineering application prospects

Based on the above analysis, Expanded Perlite Foamed Concrete (EP-FRC) demonstrates significant advantages in engineering applications due to its lightweight nature (density ~1000 kg/m<sup>3</sup>), relatively high strength, and excellent thermal insulation properties. It is particularly suitable for scenarios such as prefabricated exterior wall insulation panels (enabling integrated structure and insulation), roof insulation and leveling layers (reducing load and enhancing energy efficiency), and lightweight partition panels (improving the thermal environment and reducing construction costs). Through optimized mix design, this material exhibits clear economic benefits in both direct manufacturing costs and long-term operational energy savings, providing a solid foundation for its large-scale application in green building construction.

## 3.7. Discussion

Unlike optimization methods that follow the grading curve, the use of single size aggregates has significant deficiencies in concrete. Single size aggregates, whether large, medium or small, do not allow for effective filling between particles, resulting in high void content and insufficient densification within the concrete. This can lead to increased demand for cement paste, reduced concrete strength, and potentially poor workability. Therefore, single-size aggregates are difficult to meet the combined requirements of concrete for low void fraction, high densification, excellent strength and good workability.

In this experiment, combinations of expanded perlite aggregates with gradation indices  $q$  of 0.2, 0.3, and 0.4 were set up to investigate their theoretical effect on aggregate packing density. A lower  $q$  value (0.2) signifies a gradation curve shifted towards finer particles, leading to a significantly increased proportion of fine particles in the mixture. These finer particles effectively fill the interstitial voids between coarse ones, theoretically increasing packing density and decreasing overall void content. Conversely, an abundance of fine particles also brings disadvantages, including a significantly higher specific surface area that requires more water for wetting and hydration and may lead to increased water demand, detrimentally affecting slurry fluidity.

Furthermore, the  $q$ -value influences the quality of the Interface Transition Zone (ITZ) between the expanded perlite aggregate and the cement matrix. More fine particles from a lower  $q$ -value help to fill the tiny pores and irregularities on the expanded perlite surface, improve the contact between the cement paste and aggregate, and form a denser ITZ, which improves the interfacial bond strength, which may be another reason for the higher compressive strength at  $q$ -values close to 0.2. However, the optimization of ITZ is a complex process, and too many fine particles may also be enriched at the interface, which reduces the bond strength instead.

Microstructural analysis indicates that varying  $q$  values significantly influence the distribution of expanded perlite particles within the cement matrix, as well as the characteristics of the aggregate-matrix interface. When the  $q$ -value was close to 0.2, the observed pore structure was characterized by moderate size and uniform distribution. Uniformly distributed small-sized pores can disperse stresses more effectively and reduce stress concentration, thus enhancing strength. Therefore, the selection of the gradation index  $q$  needs to be a trade-off between optimizing the microstructure of the material to enhance the strength and constructing a more efficient insulating pore network to meet the needs of specific engineering applications.

#### 4. Conclusion

To investigate the influence of expanded perlite aggregate particle size and gradation on foamed concrete properties and its potential for engineering applications, this study conducted a systematic experimental investigation under varying water-cement ratio conditions. By comparing the properties with those of traditional foamed concrete benchmark samples, the key role of expanded perlite aggregate and its mechanism for performance regulation were revealed. The main conclusions drawn from this research are as follows.

- A key factor influencing the dry density and water absorption of expanded perlite foamed concrete is the water-cement ratio. Higher water-cement ratios resulted in a significant decrease in dry density and a considerable increase in water absorption. For a water-cement ratio increase from 0.6 to 0.8, dry density decreased from an average of  $1130.6 \text{ kg/m}^3$  to  $972.5 \text{ kg/m}^3$ , accompanied by a simultaneous increase in water absorption from 17.5 % to 23.0 %. Relative to the control group lacking expanded perlite, the material's dry density was significantly increased by expanded perlite addition, but water absorption was generally decreased at corresponding water-cement ratios. This latter effect was related to the expanded perlite aggregate's modulation of the internal pore structure (e.g., reduction in connecting pores).
- Across all water-cement ratio conditions, the 0.5–1 mm single expanded perlite aggregate exhibited the most superior compressive performance, achieving a peak strength of 9.12 MPa at a water-cement ratio of 0.6. Among the multi-particle size combinations, the 30:40:30 blend showed the second-best compressive strength overall (8.06 MPa at w/c = 0.6), attributed to its optimized particle size distribution enabling an effective balance between strength and compactness. Overall, incorporating expanded perlite aggregate greatly enhanced the mechanical strength compared to the conventional foamed concrete benchmark; expanded perlite foamed concrete consistently exhibited significantly higher compressive strength than pure foamed concrete without aggregates across all tested water-cement ratios, proving the effectiveness of expanded perlite aggregates in building a stronger internal skeleton structure and enhancing load-carrying capacity.
- A decreasing trend in overall thermal conductivity is observed with increasing water-cement ratio from 0.6 to 0.8, indicating that enhanced thermal insulation is not facilitated by lower water-cement ratios. Concerning the effect of particle size, among the single particle sizes, the 1–3 mm aggregate shows the minimum thermal conductivity (0.1303 W/(m·K)). The use of multi-particle size combinations facilitates a further reduction in thermal conductivity; the 30:40:30 combination showed the optimal thermal insulation performance at a water-cement ratio of 0.7, registering a thermal conductivity of 0.1194 W/(m·K). Nevertheless, relative to the plain foamed concrete benchmark, the thermal conductivity of expanded perlite foamed concrete is typically higher, with even the minimum thermal conductivity obtained (0.1194 W/(m·K)) being greater than the benchmark's lowest value (0.0829 W/(m·K)). This indicates that the inclusion of expanded perlite aggregate raises the solid heat transfer path, consequently reducing thermal insulation relative to a pure foam structure.
- Analysis of the microstructure indicated that the incorporation of expanded perlite aggregate and its particle size grading notably modified the material's pore structure and distribution, thereby creating a multilevel pore network that directly impacted the material's macroscopic properties. The findings of this research confirm that by precisely controlling the particle size and grading of expanded perlite aggregate, significantly improving the mechanical strength of foamed concrete is possible while preserving its beneficial lightweight and some thermal insulation properties (surpassing ordinary concrete).

This study demonstrates that the particle size and gradation of expanded perlite aggregate significantly influence the performance of foam concrete, providing a solid theoretical basis for its engineering applications in building energy conservation. The findings offer reference for engineers designing mix proportions to meet strength or thermal insulation requirements. By establishing quantitative relationships between water-cement ratio, gradation, and performance, targeted parameter adjustments can be achieved. However, the application of expanded perlite still faces challenges, primarily manifested in the trade-off between strength and thermal insulation performance, the brittleness and high water absorption of the aggregate, as well as production costs and stable supply issues. To more comprehensively evaluate its application potential, future research will focus on its durability and sustainability. We will prioritize experiments on key durability parameters such as water resistance and freeze-thaw cycle resistance to better understand the material's long-term performance in complex environments. This will comprehensively demonstrate its value as a green, sustainable building material at the macro level. Future research will extend beyond enhancing fundamental properties to encompass integrated performance evaluations, thereby driving its practical application in building energy efficiency.

#### CRediT authorship contribution statement

**Yandong Liu:** Writing – original draft, Methodology, Formal analysis, Conceptualization. **Lingyonxg Ma:** Visualization, Software, Investigation. **Wei Jiang:** Writing – review & editing, Supervision. **Qing Li:** Resources, Project administration. **Ming Qiao:** Investigation, Data curation. **Shijie Fan:** Validation, Methodology. **Dong Li:** Writing – review & editing, Funding acquisition.

#### Funding

Financial support was provided by the Natural Science Foundation of Heilongjiang Province of China (Grant No. LH2024E104), Provincial Science Fund for Distinguished Young Scholars of Heilongjiang Provience of China (Grant No. JQ2024E001), Provincial Science and Technology Innovation Base Award Project of China (Grant No. GY2024JD0005) and the China Postdoctoral Science

Foundation (Grant No. 2024MD763936).

### Declaration of competing interest

The authors declare that they have no known competing financial interests or personal relationships that could have appeared to influence the work reported in this paper.

### Data availability

Data will be made available on request.

### References

- [1] A. Ullah, H. Nobanee, S. Ullah, H. Iftikhar, Renewable energy transition and regional integration: energizing the pathway to sustainable development, *Energy Policy* 193 (2024) 114270, <https://doi.org/10.1016/j.enpol.2024.114270>.
- [2] P. Naghipour, A. Naghipour, Energy performance analysis of residential buildings in Bandar Anzali: influence of orientation and aspect ratio, *Sustainability* 5 (2025) 100140, <https://doi.org/10.1016/j.nxust.2025.100140>.
- [3] S.K. Depren, M.T. Kartal, N.C. Çelikdemir, Ö. Depren, Energy consumption and environmental degradation nexus: a systematic review and meta-analysis of fossil fuel and renewable energy consumption, *Ecol. Inform.* 70 (2022) 101747, <https://doi.org/10.1016/j.ecoinf.2022.101747>.
- [4] P. Naghipour, A. Naghipour, A.H. Shirdel, et al., Sustainability in historical Islamic architecture: lessons from Sheikh Lotfollah Mosque's construction techniques, *Journal of Islamic Architecture* 8 (2025) 585–603, <https://doi.org/10.18860/jia.v8i3.29053>.
- [5] P. Naghipour, A. Naghipour, Evaluating heating energy consumption in residential buildings using hybrid machine learning models: the case of Parsabad City, *Research* (2025) 100721, <https://doi.org/10.1016/j.nexres.2025.100721>.
- [6] E. Aydin, D. Brounen, The impact of policy on residential energy consumption, *Energy* 169 (2019) 115–129, <https://doi.org/10.1016/j.energy.2018.12.030>.
- [7] A. Zakari, I. Khan, D. Tan, R. Alvarado, V. Dagar, Energy efficiency and sustainable development goals (SDGs), *Energy* 239 (2022) 122365, <https://doi.org/10.1016/j.energy.2021.122365>.
- [8] Z. Xiaosan, J. Qingquan, K.S. Iqbal, A. Manzoor, R.Z. Ur, Achieving sustainability and energy efficiency goals: assessing the impact of hydroelectric and renewable electricity generation on carbon dioxide emission in China, *Energy Policy* 155 (2021) 112332, <https://doi.org/10.1016/j.enpol.2021.112332>.
- [9] N.P. Tran, T.N. Nguyen, T.D. Ngo, P.K. Le, T.A. Le, Strategic progress in foam stabilisation towards high-performance foam concrete for building sustainability: a state-of-the-art review, *J. Clean. Prod.* 375 (2022) 133939, <https://doi.org/10.1016/j.jclepro.2022.133939>.
- [10] F. Wu, Q. Niu, X. Chen, Y. Guo, Resource utilization of antimony tailings: preparation of lightweight, waterproof and environmental friendly foamed concrete, *Sustain. Chem. Pharm.* 43 (2025) 101907, <https://doi.org/10.1016/j.scp.2025.101907>.
- [11] L. Hou, J. Li, Z. Lu, Y. Niu, Influence of foaming agent on cement and foam concrete, *Constr. Build. Mater.* 280 (2021) 122399, <https://doi.org/10.1016/j.conbuildmat.2021.122399>.
- [12] A.I. Çelik, U. Tunç, R. Kayabaşı, M.C. Acar, A. Şener, Y.O. Özklıci, Influence of aluminum waste, hydrogen peroxide, and silica fume ratios on the mechanical and thermal characteristics of alkali-activated sustainable raw perlite based geopolymers paste, *Sustain. Chem. Pharm.* 41 (2024) 101727, <https://doi.org/10.1016/j.scp.2024.101727>.
- [13] O. Gencel, O.Y. Bayraktar, G. Kaplan, O. Arslan, M. Nodehi, A. Benli, T. Ozbakaloglu, Lightweight foam concrete containing expanded perlite and glass sand: physico-mechanical, durability, and insulation properties, *Constr. Build. Mater.* 320 (2022) 126187, <https://doi.org/10.1016/j.conbuildmat.2021.126187>.
- [14] R. Demirboğa, R. Gül, Thermal conductivity and compressive strength of expanded perlite aggregate concrete with mineral admixtures, *Energy Build.* 35 (11) (2003) 1155–1159, <https://doi.org/10.1016/j.enbuild.2003.09.002>.
- [15] O. Sengul, S. Azizi, F. Karaosmanoglu, M.A. Tasdemir, Effect of expanded perlite on the mechanical properties and thermal conductivity of lightweight concrete, *Energy Build.* 43 (2–3) (2011) 671–676, <https://doi.org/10.1016/j.enbuild.2010.11.008>.
- [16] L. Wang, P. Liu, Q. Jing, Y. Liu, W. Wang, Y. Zhang, Z. Li, Strength properties and thermal conductivity of concrete with the addition of expanded perlite filled with aerogel, *Constr. Build. Mater.* 188 (2018) 747–757, <https://doi.org/10.1016/j.conbuildmat.2018.08.054>.
- [17] M. Ibrahim, A. Ahmad, M.S. Barry, L.M. Alhems, A.C. Mohamed Suhoothi, Durability of structural lightweight concrete containing expanded perlite aggregate, *Int. J. Concr. Struct. Mater.* 14 (2020) 1–15, <https://doi.org/10.1186/s40069-020-00425-w>.
- [18] S. Grzeszczyk, G. Janus, Lightweight reactive powder concrete containing expanded perlite, *Materials* 14 (12) (2021) 3341, <https://doi.org/10.3390/mater14123341>.
- [19] G. Jia, Z. Li, Influence of the aerogel-expanded perlite composite as thermal insulation aggregate on the cement-based materials: preparation, property, and microstructure, *Constr. Build. Mater.* 273 (2021) 121728, <https://doi.org/10.1016/j.conbuildmat.2020.121728>.
- [20] S.M. Alexa-Stratulat, G. Tararu, A.M. Toma, I. Olteanu, C. Pastia, G. Bunea, I.O. Toma, Effect of expanded perlite aggregates and temperature on the strength and dynamic elastic properties of cement mortar, *Constr. Build. Mater.* 438 (2024) 137229, <https://doi.org/10.1016/j.conbuildmat.2024.137229>.
- [21] D. Sarı, A.G. Pasamehmetoglu, The effects of gradation and admixture on the pumice lightweight aggregate concrete, *Cem. Concr. Res.* 35 (5) (2005) 936–942, <https://doi.org/10.1016/j.cemconres.2004.04.020>.
- [22] International Organization for Standardization, Testing of concrete — part 4: strength of hardened concrete, ISO 1920-4:2020 (2020), <https://doi.org/10.3403/30367557>. ISO 1920-4:2020.
- [23] ASTM International, Standard Test Method for steady-state Thermal Transmission Properties by Means of the Heat Flow Meter Apparatus (ASTM C518-21), ASTM C518-21, 2021, <https://doi.org/10.1520/c0518-17>.
- [24] L.H. Nguyen, A.L. Beaucour, S. Ortola, et al., Experimental study on the thermal properties of lightweight aggregate concretes at different moisture contents and ambient temperatures, *Constr. Build. Mater.* 151 (2017) 720–731, <https://doi.org/10.1016/j.conbuildmat.2017.06.087>.
- [25] Md Azree Othuman Mydin, et al., Performance of lightweight foamed concrete partially replacing cement with industrial and agricultural wastes: microstructure characteristics, thermal conductivity, and hardened properties, *Ain Shams Eng. J.* 14 (2023) 102546, <https://doi.org/10.1016/j.asej.2023.102546>.
- [26] J. Dai, Q. Wang, X. Lou, X. Bao, B. Zhang, J. Wang, X. Zhang, Solution calorimetry to assess effects of water-cement ratio and low temperature on hydration heat of cement, *Constr. Build. Mater.* 269 (2021) 121222, <https://doi.org/10.1016/j.conbuildmat.2020.121222>.
- [27] X. Ou, B. Liao, J. Jiang, M. Chen, F. Chen, L. Huang, Effect of water-cement ratio on the bond strength of cold joint foam concrete and crack evolution characteristics, *J. Build. Eng.* 95 (2024) 110267, <https://doi.org/10.1016/j.jobe.2024.110267>.
- [28] Y. Yan, W. Liu, Z. Li, G. Jia, Y. Zhang, G. Ma, Y. Gao, Mechanical properties and frost resistance of self-healing concrete based on expanded perlite with different particle sizes as microbial carrier, *Constr. Build. Mater.* 422 (2024) 135450, <https://doi.org/10.1016/j.conbuildmat.2024.135450>.
- [29] X. Wang, D. Wu, Q. Geng, D. Hou, M. Wang, L. Li, Z. Sun, Characterization of sustainable ultra-high performance concrete (UHPC) including expanded perlite, *Constr. Build. Mater.* 303 (2021) 124245, <https://doi.org/10.1016/j.conbuildmat.2021.124245>.
- [30] J. Sun, J. Zhao, W. Zhang, J. Xu, B. Wang, X. Wang, Y. Liu, Composites with a novel core-shell structural expanded perlite/polyethylene glycol composite PCM as novel green energy storage composites for building energy conservation, *Appl. Energy* 330 (2023) 120363, <https://doi.org/10.1016/j.apenergy.2022.120363>.

- [31] O. Benjeddou, G. Ravindran, M.A. Abdelzaher, Thermal and acoustic features of lightweight concrete based on marble wastes and expanded perlite aggregate, *Buildings* 13 (4) (2023) 992, <https://doi.org/10.3390/buildings13040992>.
- [32] X. Zhang, D. Pan, G. Zhu, Preparation and characterization of form-stable phase-change materials with enhanced thermal conductivity based on nano-Al<sub>2</sub>O<sub>3</sub> modified binary fatty acids and expanded perlite, *Energy Build.* 271 (2022) 112330, <https://doi.org/10.1016/j.enbuild.2022.112330>.
- [33] Y. Yan, W. Liu, G. Jia, Y. Zhang, Y. Gao, Z. Li, Application of expanded perlite immobilized microorganisms in cementitious materials, *J. Build. Eng.* 76 (2023) 106834, <https://doi.org/10.1016/j.conbuildmat.2024.135450>.